Contribution from the Department of Chemistry,
University of Minnesota, Minneapolis, Minnesota 55455

Effect of Arene Substituents and Temperature on the Arene Replacement Reactions of $[(\eta^5\text{-}C_5H_5)Fe(\eta^6\text{-arene})]^+$ and $[(\eta^5\text{-}C_5H_5)Ru(\eta^6\text{-arene})]^+$

AMY M. McNAIR, JANET L. SCHRENK, and KENT R. MANN*

Received January 26, 1984

The photochemical removal of the arene from $[(\eta^5\text{-}C_5H_5)M(\eta^6\text{-arene})]^+$ has been studied for complexes of Fe(II) and Ru(II): (Fe, arene = *p*-dichlorobenzene, benzene, toluene, toluene-d_8, *p*-xylene, mesitylene, durene, pentamethylbenzene, hexamethylbenzene, hexaethylbenzene, and tri-*tert*-butylbenzene; Ru, *p*-dichlorobenzene, benzene, toluene, mesitylene, pentamethylbenzene, hexamethylbenzene, and tri-*tert*-butylbenzene). The photoactive state in these complexes has been identified as the distorted a^3E_1 ligand field excited state. A linear correlation exists between log $(\phi/(1-\phi))$ and σ_p, the Hammett parameter for chloro- and methylarene substituted complexes (up to five substituents for Fe and six substituents for Ru). The Hammett ρ parameter is +1.03 and +0.53 for for the Fe complexes in CH_2Cl_2 and CH_3CN solution, respectively; for the Ru complexes in CH_3CN solution ρ = +1.38. These data indicate a small amount of negative charge builds up at the arene in the transition state for the arene release reaction in these systems. Deviations from the linear correlation of log $(\phi/(1-\phi))$ with σ_p were found for the sterically hindered $[(\eta^5\text{-}C_5H_5)Fe(\eta^6\text{-hexamethylbenzene})]^+$, $[(\eta^5\text{-}C_5H_5)Fe(\eta^6\text{-hexaethylbenzene})]^+$, and $[(\eta^5\text{-}C_5H_5)Fe(\eta^6\text{-1,3,5-tri-}tert\text{-butylbenzene})]^+$ complexes. These deviations result from the steric interactions which hinder the participation of anions and solvent molecules in the transition state. The temperature dependence of photochemical arene release from $[(\eta^5\text{-}C_5H_5)M(\eta^6\text{-arene})]X$ (M = Fe, arene = *p*-xylene, hexamethylbenzene, X^- = BF_4^-, solvent = CH_2Cl_2, CH_3CN; M = Ru, arene = benzene, X^- = PF_6, solvent = CH_3CN) has been investigated. Plots of log $(\phi/(1-\phi))$ vs. $1/T$ are linear in all cases. From the slopes of these lines the difference in the apparent activation energies ($E_{a,p} - E_{a,nr}$) between the product-forming step and the nonradiative decay of the a^3E_1 excited state are 1.0–3.6 kcal/mol. These studies indicate that the M–arene bond is nearly broken in the a^3E_1 excited state. Medium effects on the most sterically hindered Fe complexes investigated ($[(\eta^5\text{-}C_5H_5)Fe(\eta^6\text{-hexamethylbenzene})]^+$ and $[(\eta^5\text{-}C_5H_5)Fe(\eta^6\text{-hexaethylbenzene})]^+$) show that a limiting value of about 0.0007 occurs for the quantum yield of arene release for $[(\eta^5\text{-}C_5H_5)Fe(\eta^6\text{-hexaethylbenzene})]^+$ in CH_2Cl_2 solutions with AsF_6^- present. This quantum yield represents an upper limit of the dissociative arene release for the $[(\eta^5\text{-}C_5H_5)Fe(\eta^6\text{-arene})]^+$ systems.

Introduction

Preliminary experimental work[1] from our laboratory concerning the photochemically initiated arene replacement reactions of $[(\eta^5\text{-}C_5H_5)Fe(\eta^6\text{-}p\text{-xyl})]^+$ and $[(\eta^5\text{-}C_5H_5)Ru(\eta^6\text{-}C_6H_6)]^+$ (xyl = xylene, C_6H_6 = benzene) by substituted phosphites ($P(OR)_3$, R = methyl, ethyl, isopropyl, phenyl) suggested that considerable mechanistic differences exist between the Fe and Ru systems. We speculated that the strong *dependence* of the quantum yield ϕ on the nature of the phosphite substituent in the Ru system was the result of nucleophilic attack of $P(OR)_3$ at the excited metal center prior to arene release, while the *independence* exhibited by ϕ on phosphite substituent in the Fe system was due to dissociative character in the arene release reaction. Our analysis of these results assumed no involvement of the very weakly nucleophilic medium (CH_2Cl_2) in the reactions of the Fe system.

More recently completed work[2] suggests this assumption is untenable. Experiments indicate photochemical arene replacement reactions of $[(\eta^5\text{-}C_5H_5)Fe(\eta^6\text{-}p\text{-xylene})]^+$ occur via a mechanism that involves a medium-assisted step. The assistance depends on solvent ($CH_2Cl_2 < CH_3CN < CH_3OH < H_2O <$ propylene carbonate) and counterion ($CF_3SO_3^- > BF_4^- > Br^- \approx ClO_4^- >> PF_6^- \approx AsF_6^- \approx SbF_6^-$) in a manner characteristic of the mechanism exhibited by the phosphite–Ru system. The arene replacement reactions of $[(\eta^5\text{-}C_5H_5)Fe(\eta^6\text{-}p\text{-xyl})]^+$ occur via nucleophilic attack of the solvent cage or an ion-paired anion on an excited state of $[(\eta^5\text{-}C_5H_5)Fe(\eta^6\text{-}p\text{-xyl})]^+$.

The investigations reported here identify the photoactive excited state, delineate substituent effects, and determine the temperature dependence of the quantum yield for a series of substituted arene $[(\eta^5\text{-}C_5H_5)Fe(\eta^6\text{-arene})]^+$ and $[(\eta^5\text{-}C_5H_5)Ru(\eta^6\text{-arene})]^+$ complexes. These studies indicate metal–arene bond cleavage for complexes of both metals is nearly complete in the reactive excited state, but nucleophilic interactions of the medium in the transition state ultimately control the quantum yield of arene release for a given complex.

Experimental Section

General Considerations. Dichloromethane and acetonitrile were of spectroscopic grade and were dried over activated alumina or activated 4-Å molecular sieves prior to use. $NaBF_4$, NH_4PF_6, $NaSbF_6$, and H_3OAsF_6 were purchased from Southwestern Analytical Chemicals. HSO_3CF_3 was obtained as a gift from the 3M Co. (TBA)SO_3CF_3, (TBA)AsF_6, and (TBA)SbF_6 (TBA = tetra-*n*-butylammonium) were available from a previous study.[2] All other reagents were purchased as reagent grade and used as received. UV–visible spectra were obtained on a Cary 17D spectrophotometer. ^1H NMR spectra were obtained on acetone-d_6 solutions of the compounds with a Varian CFT 20 spectrometer equipped with a proton accessory.

Synthesis of $[(\eta^5\text{-}C_5H_5)Fe(\eta^6\text{-arene})]X$ Compounds. The Fe compounds were synthesized as described previously by a modification of the method of Nesmeyanov et al.[3,4] The various salts of the compounds containing the $[(\eta^5\text{-}C_5H_5)Fe(\eta^6\text{-arene})]^+$ cations used in this study were obtained by adding a simple salt containing the desired anion to the aqueous solutions of the cations available from the synthetic procedure. All the compounds with the exception of $[(\eta^5\text{-}C_5H_5)Fe(\eta^6\text{-1,3,5-}(t\text{-Bu})_3C_6H_3)]BF_4$ and $[(\eta^5\text{-}C_5H_5)Fe(\eta^6\text{-tol-}d_8)]PF_6$ contain cations that have been reported previously.[5]

$[(\eta^5\text{-}C_5H_5)Fe(\eta^6\text{-1,3,5-}(t\text{-Bu})_3C_6H_3)]BF_4$ (1,3,5-(*t*-Bu)$_3C_6H_3$ = 1,3,5-tri-*tert*-butylbenzene): mp 200 °C dec; ^1H NMR δ 6.46 (s, aromatic protons, 3 H), 5.22 (s, Cp, 5 H), 1.55 (s, CH_3, 27 H). Anal. Calcd for $C_{23}H_{35}FeBF_4$: C, 60.82; H, 7.77. Found: C, 60.59, H, 7.87.

(1) Gill, T. P.; Mann, K. R. *Organometallics* **1982**, *1*, 485.
(2) Schrenk, J. L.; Palazzotto, M. C.; Mann, K. R. *Inorg. Chem.* **1983**, *22*, 4047.
(3) (a) Nesmeyanov, A. N.; Vol'kenau, N. A.; Bolesova, I. N. *Dokl. Akad. Nauk SSSR* **1963**, *149*, 615. (b) Nesmeyanov, A. N.; Vol'kenau, N. A.; Bolesova, I. N. *Tetrahedron Lett.* **1963**, 1725.
(4) Roman, E.; Astruc, D. *Inorg. Chem.* **1979**, *18*, 3284.
(5) (a) Sutherland, R. G. *J. Organomet. Chem. Libr.* **1977**, *3*, 311. (b) Khand, I. U.; Pauson, P. L.; Watts, W. E. *J. Chem. Soc. C* **1968**, 2257. (c) Khand, I. U. *Ibid.* **1968**, 2261. (d) Astruc, D.; Hamon, J.-R.; Althoff, G.; Roman, E.; Batail, P.; Michaud, P.; Mariot, J.-P.; Varret, F.; Cozak, D. *J. Am. Chem. Soc.* **1979**, *101*, 5445. (e) Hamon, J.-R.; Saillard, J.-Y.; Beuze, A. L.; McGlinchey, M. J.; Astruc, D. *Ibid.* **1982**, *104*, 7549.

0020-1669/84/1323-2633$01.50/0 © 1984 American Chemical Society

$[(\eta^5\text{-}C_5H_5)Fe(\eta^6\text{-tol-}d_8)]PF_6$ (tol = toluene): mp 140 °C dec; ^1H NMR δ 5.17 (s, Cp, 5 H). ^1H NMR indicates that the toluene moiety is approximately 96% deuterated.

Synthesis of $[(\eta^5\text{-}C_5H_5)Ru(\eta^6\text{-arene})]X$ Compounds. $[(\eta^5\text{-}C_5H_5)Ru(\eta^6\text{-}C_6H_6)]PF_6$ was prepared by a literature procedure.[6] The other compounds ($[\eta^5\text{-}C_5H_5)Ru(\eta^6\text{-arene})]PF_6$, arene = benzene-$d_6$ (C_6D_6), *p*-dichlorobenzene (*p*-$Cl_2C_6H_4$), toluene, mesitylene (mes) pentamethylbenzene (PMB), hexamethylbenzene (HMB), and tri-*tert*-butylbenzene) were synthesized from $[(\eta^5\text{-}C_5H_5)Ru(CH_3CN)_3]PF_6$.[1] The *p*-dichlorobenzene, mesitylene, and hexamethylbenzene complexes have been characterized.[7]

$[(\eta^5\text{-}C_5H_5)Ru(\eta^6\text{-tol})]PF_6$: mp 295–296 °C dec; ^1H NMR δ 6.29 (s, aromatic protons, 5 H), 5.50 (s, Cp, 5 H), 2.42 (s, CH_3, 3 H). Anal. Calcd for $C_{12}H_{13}RuPF_6$: C, 35.74; H, 3.25. Found: C, 35.55, H, 3.34.

$[(\eta^5\text{-}C_5H_5)Ru(\eta^6\text{-PMB})]PF_6$: mp 322–325 dec; ^1H NMR δ 6.28 (s, aromatic protons, 1 H), 5.25 (s, Cp, 5 H), 2.50 (s, CH_3, 3 H), 2.43 (s, CH_3, 6 H), 2.41 (s, CH_3, 6 H). Anal. Calcd for $C_{16}H_{21}RuPF_6$: C, 41.83; H, 4.61. Found: C, 41.75; H, 4.79.

$[(\eta^5\text{-}C_5H_5)Ru(\eta^6\text{-1,3,5-}(t\text{-Bu})_3C_6H_3)]PF_6$: mp 289–290 °C dec; ^1H NMR δ 6.46 (s, aromatic protons, 3 H), 5.57 (s, Cp, 5 H), 1.42 (s, CH_3, 27 H). Anal. Calcd for $C_{23}H_{35}RuPF_6$: C, 49.54; H, 6.33. Found: C, 49.61; H, 6.34.

$[(\eta^5\text{-}C_5H_5)Ru(\eta^6\text{-}C_6D_6)]PF_6$: mp 325–326 °C dec; ^1H NMR δ 5.53 (s, Cp, 5 H). Anal. Calcd for $C_{11}H_5D_6RuPF_6$: C, 33.42; H, 2.97 (H percentage is the mass weighted average). Found: C, 33.39; H, 2.69 (determined as mass weighted average). ^1H NMR indicates that the benzene moiety is approximately 99% deuterated.

Compound Purification. The compounds were purified by dissolving them in dichloromethane (Fe) or acetone (Ru) and passing the solutions down a short alumina column. The solutions were then evaporated to yield microcrystalline powders. All operations were carried out in the dark for the Fe compounds.

Photolysis Procedures. General Considerations. Monochromatic light was obtained from the output of a 100-W medium-pressure mercury lamp with the appropriate interference filter (Oriel). The monochromatic light beam was then passed into sealed quartz (Ru) or Pyrex (Fe) cells, which were held in a cell holder consisting of an insulated copper block mounted on a magnetic stirrer. The temperature of the photolysis cell was controlled (±0.5 °C) by circulating thermostated isopropyl alcohol through the copper block. The temperature was monitored with a copper–constantan thermocouple immersed in the photolysis solution. All solutions were stirred during photolysis.

Quantum Yield Procedures for the Fe Compounds. Quantum yields (λ_{irr} = 436 nm) were measured for the appearance of the $Fe(phen)_3^{2+}$ complex according to the stoichiometry of reaction 1.

$$[(\eta^5\text{-}C_5H_5)Fe(\eta^6\text{-arene})]^+ \xrightarrow{h\nu} Fe(phen)_3^{2+} + \text{arene} + C_5H_5^- \quad (1)$$

The method used in making these measurements has been described previously.[8] Briefly, it corrects for inner filter and incomplete light absorption effects[9] and utilizes the previously investigated $[(\eta^5\text{-}C_5H_5)Fe(\eta^6\text{-}p\text{-xyl})]BF_4$ complex as the actinometer.[2] The quantum yield data reported for the Fe compounds are the average of at least three independent measurements. The relative precision of the measurements averages 4%; the absolute accuracy of the measurements is traceable to the accuracy of the Reineckate actinometry[10] used to determine the quantum yield of $[(\eta^5\text{-}C_5H_5)Fe(\eta^6\text{-}p\text{-xyl})]BF_4$.

Quantum Yield Procedures for the Ru Compounds. Quantum yields (λ_{irr} = 313 nm) were measured for degassed, stirred solutions of the $[(\eta^5\text{-}C_5H_5)Ru(\eta^6\text{-arene})]^+$ complexes. The appearance of $[(\eta^5\text{-}C_5H_5)Ru(CH_3CN)_3]^+$ was conveniently monitored as previously described for the benzene complex.[1] Quantum yields are based on the stoichiometry of eq 2. The procedure for determining the quantum

$$[(\eta^5\text{-}C_5H_5)Ru(\eta^6\text{-arene})]^+ \xrightarrow[CH_3CN]{h\nu} [(\eta^5\text{-}C_5H_5)Ru(CH_3CN)_3]^+ + \text{arene} \quad (2)$$

Table I. Electronic Absorption Spectra[a] of $[(\eta^5\text{-}C_5H_5)Fe(\eta^6\text{-arene})]^+$ Complexes

arene	λ_{max} (ϵ_{max})[b]			
	CH_2Cl_2		CH_3CN	
p-dichlorobenzene	390 (100)	457 (65)	388 (104)	465 (61)
chlorobenzene	386 (87)	385 (84)	385 (84)	443 (62)
benzene	382 (88)	452 (61)		
toluene	386 (76)	451 (59)	386 (75)	450 (61)
p-xylene	390 (86)	450 (69)	387 (86)	446 (65)
mesitylene	391 (91)	442 (68)	393 (85)	442 (64)
durene	397 (90)	468 (63)[c]	396 (90)	466 (63)[c]
pentamethylbenzene	400 (88)	470 (60)[c]	399 (89)	468 (66)[c]
hexamethylbenzene	403 (82)	470 (60)[c]	403 (78)	469 (58)[c]
1,3,5-tri-*tert*-butylbenzene	404 (79)	477 (49)[c]		
hexaethylbenzene	404 (79)	457 (72)	401 (72)	456 (66)

[a] Determined at 25 °C. [b] Wavelength (λ) in nm; extinction coefficient (ϵ) in M^{-1} cm^{-1} (±10%). [c] Shoulder.

yield for each compound involved measuring the absorption spectrum (280–600 nm) as a function of photolysis time (five to eight data points) for one to three independently prepared solutions. The data for a given solution were corrected for incomplete light absorption and inner filter effects.[9] Actinometric measurements were made periodically with the Reineckate[10] actinometer. Quantum yields were calculated as the average of all the data obtained for each compound (a minimum of five data points).

Sensitization Studies. The arene release reaction of 0.002 M $[(\eta^5\text{-}C_5H_5)Fe(\eta^6\text{-}p\text{-xyl})]BF_4$ was sensitized in degassed CH_2Cl_2 solutions with 0.15 M benzil (E_T = 18 800 cm^{-1})[11] and 0.03 M anthracene (E_T = 14 700 cm^{-1}).[12] Both sensitizers were irradiated with 366-nm light (interference filter). Small corrections were made for the direct photolysis of the weakly absorbing Fe complex. The amount of arene release was estimated by adding 1,10-phenanthroline to the solutions after photolysis. Quantum yields were not measured.

Long-Wavelength Photolyses. The photolyses of 0.02 M $[(\eta^5\text{-}C_5H_5)Fe(\eta^6\text{-}p\text{-xyl})]BF_4$ (578 and 690 nm, interference filters) in CH_2Cl_2 solution and 0.04 M $[(\eta^5\text{-}C_5H_5)Ru(\eta^6\text{-}C_6H_6)]PF_6$ (406 nm, interference filter) in CH_3CN solution were carried out in the same manner as the short-wavelength experiments, except the photolysis times were increased to compensate for the low extinction coefficients of the compounds at these wavelengths. Quantum yields were not measured.

Thermal Control Reactions. Solutions of the Fe and Ru compounds stored in the dark at 25 °C were monitored by UV–visible spectroscopy. No dark reactions were found for any of the compounds on the photolysis time scales.

Conductivity Measurements. Conductivities were measured for salts of the $[(\eta^5\text{-}C_5H_5)Fe(\eta^6\text{-HEB})]^+$ cation (HEB = hexaethylbenzene) by a method previously described.[2]

Thermal Activation Energy for *p*-Xylene Release from $[(\eta^5\text{-}C_5H_5)Fe(\eta^6\text{-}p\text{-xyl})]BF_4$. A solution of 0.02 M $[(\eta^5\text{-}C_5H_5)Fe(\eta^6\text{-}p\text{-xyl})]BF_4$ in acetonitrile was held at 60 °C for 5 h. After the reaction was quenched, 1,10-phenanthroline was added to the solution. Absorbance measurements of this solution at 510 nm indicated that less than 6.76×10^{-6} M $Fe(phen)_3^{2+}$ (our previously estimated detection limit) was formed. An upper limit for the first-order rate constant at 333 K of $k_{333\,K} = 2 \times 10^{-8}$ s^{-1} is calculated. By use of the previously[8] estimated value of $k_{298\,K} = 4 \times 10^{-10}$ s^{-1} and the Arrhenius equation, an E_a value of 22 kcal/mol is estimated for the thermal arene release reaction. This is a very approximate value, due to the large uncertainties in the rate constants measured.

Results

UV–Vis Absorption Spectra. Absorption spectra for the Fe and Ru complexes were recorded in the ligand field (LF) spectral region under several different experimental conditions. These data are reported in Tables I–III.

(6) Zelonka, R. A.; Baird, M. C. *J. Organomet. Chem.* **1972**, *44*, 383.
(7) Roman, E.; Astruc, D. *Inorg. Chim. Acta* **1979**, *37*, L465.
(8) Gill, T. P.; Mann, K. R. *Inorg. Chem.* **1980**, *19*, 3007.
(9) Kling, O.; Nikoaiski, E.; Schlafer, H. L. *Ber. Bunsenges. Phys. Chem.* **1963**, *67*, 883.
(10) Wegner, E. E.; Adamson, A. W. *J. Am. Chem. Soc.* **1966**, *88*, 394.
(11) Herkstroeter, W. A.; Lamola, A. A.; Hammond, G. S. *J. Am. Chem. Soc.* **1964**, *86*, 4537.
(12) Birks, J. B. "Photophysics of Aromatic Molecules"; Wiley-Interscience: New York, 1970; p 182.

Table II. Electronic Absorption Spectra[a] of $[(\eta^5\text{-}C_5H_5)Fe(\eta^6\text{-arene})]^+$ Complexes as a Function of Anion and Solvent

arene	anion	solvent/ electrolyte	λ_{max} (ϵ_{max})[b]	
p-xylene	$CF_3SO_3^-$	CH_2Cl_2	390 (84)	449 (67)
p-xylene	PF_6^-	CH_2Cl_2	390 (84)	449 (66)
p-xylene	PF_6^-	CH_2Cl_2/0.1 M (TBA)PF_6	389 (79)	449 (61)
p-xylene	AsF_6^-	CH_2Cl_2	390 (84)	450 (65)
p-xylene	AsF_6^-	CH_2Cl_2/0.1 M (TBA)AsF_6	390 (75)	447 (58)
p-xylene	SbF_6^-	CH_2Cl_2	389 (84)	449 (64)
p-xylene	SbF_6^-	CH_3CN	388 (76)	448 (59)
p-xylene	SbF_6^-	propylene carbonate	389 (86)	448 (66)
p-xylene	SbF_6^-	CH_2Cl_2/0.1 M (TBA)SbF_6	390 (83)	448 (63)
p-xylene	SbF_6^-	CH_2Cl_2/0.1 M (TBA)ClO_4	390 (84)	448 (65)
p-xylene	SbF_6^-	CH_2Cl_2/0.1 M (TBA)Br	389 (82)	448 (64)
p-xylene	SbF_6^-	CH_2Cl_2/0.02 M (TBA)Br	389 (77)	448 (60)
p-xylene	BF_4^-	CH_2Cl_2	390 (86)	450 (69)
p-xylene	BF_4^-	CH_2Cl_2/0.1 M (TBA)BF_4	389 (84)	448 (65)
p-xylene	BF_4^-	CH_3OH	388 (97)	447 (72)
p-xylene	BF_4^-	propylene carbonate	387 (86)	448 (65)
toluene	PF_6^-	CH_2Cl_2	387 (76)	452 (62)
toluene	PF_6^-	CH_3CN	385 (73)	452 (60)
toluene-d_8	PF_6^-	CH_2Cl_2	385 (80)	449 (63)
hexaethylbenzene	PF_6^-	CH_2Cl_2	404 (79)	459 (73)
hexaethylbenzene	AsF_6^-	CH_2Cl_2	404 (80)	457 (74)
hexaethylbenzene	SbF_6^-	CH_2Cl_2	405 (78)	458 (73)
hexaethylbenzene	SbF_6^-	CH_3CN	401 (72)	456 (66)
hexaethylbenzene	BPh_4^-	CH_2Cl_2	405 (79)	457 (74)
hexaethylbenzene	BF_4^-	CH_2Cl_2/0.1 M (TBA)BF_4	403 (78)	457 (74)
hexaethylbenzene	AsF_6^-	CH_2Cl_2/0.1 M (TBA)AsF_6	404 (80)	459 (74)

[a] Determined at 25 °C. [b] Wavelength (λ) in nm; extinction coefficient (ϵ) in M^{-1} cm^{-1} (±10%).

Table III. Electronic Absorption Spectra[a] of $[(\eta^5\text{-}C_5H_5)Ru(\eta^6\text{-arene})]PF_6$ Complexes

arene	λ_{max} (ϵ_{max})[b]	
p-dichlorobenzene	330 (186)[c]	*d*
benzene	325 (144)	*d*
toluene	323 (157)	*d*
mesitylene	327 (166)[c]	*d*
pentamethylbenzene	328 (183)[c]	*d*
hexamethylbenzene	328 (170)[c]	370 (9)[c,e]
1,3,5-tri-*tert*-butylbenzene	330 (133)[c]	380 (8)[c,e,f]

[a] All spectra were determined in acetonitrile solution at 25 °C except as noted. [b] Wavelength (λ) in nm; extinction coefficient (ϵ) in M^{-1} cm^{-1} (±10%). [c] Shoulder. [d] Low solubility precludes the observation of these weak absorption bands. [e] Singlet-triplet transition observed for concentrated solutions. [f] Determined in dichloromethane solution.

Spectral assignments have been made previously for some of the Fe complexes.[13] In all cases the spectra at wavelengths longer than 360 nm exhibit an absorption peak ($\lambda_{max} \approx 390$ nm, $\epsilon_{max} \approx 85$ M^{-1} cm^{-1}) and a low-energy shoulder. The positions of both of these electronic transitions depend on the arene but are relatively independent of solvent and counterion for any given complex. These transitions[14,15] are assigned as $^1E_2 \leftarrow {}^1A_1$ (absorption peak) and $a^1E_1 \leftarrow {}^1A_1$ (shoulder) by analogy to the previously studied compounds.

Table IV. Substituent Effects on the Quantum Yield[a] for Arene Release for $[(\eta^5\text{-}C_5H_5)M(\eta^6\text{-arene})]^+$ Complexes

arene	Fe		Ru
	CH_2Cl_2	CH_3CN	CH_3CN
p-dichlorobenzene	0.90 (2)	0.88 (1)	0.61 (1)
benzene	0.75 (1)		0.34 (1)
toluene	0.63 (3)	0.79 (4)	0.17 (1)
p-xylene	0.58 (3)	0.70 (5)	
mesitylene	0.52 (3)	0.71 (1)	0.085 (4)
durene	0.47 (1)	0.67 (3)	
pentamethylbenzene	0.22 (2)	0.59 (1)	0.029 (1)
hexamethylbenzene	0.035 (2)	0.41 (1)	0.014 (1)
1,3,5-tri-*tert*-butylbenzene	0.140 (6)		0.0031 (2)
hexaethylbenzene	0.0044 (2)	0.30 (1)	

[a] Numbers in parentheses are the estimated standard deviations in the last significant digits.

The high solubility of $[(\eta^5\text{-}C_5H_5)Fe(\eta^6\text{-}p\text{-xyl})]BF_4$ allowed the singlet–triplet LF region to be investigated. Spectra obtained on highly concentrated solutions exhibit a weak transition at $\lambda_{max} \approx 650$ nm ($\epsilon_{max} \approx 1.5$ M^{-1} cm^{-1}), which we assign as the lowest singlet–triplet transition $a^3E_1 \leftarrow {}^1A_1$.[16,17] The position and intensity of this transition are also independent of solvent (CH_2Cl_2, CH_3CN).

The isoelectronic Ru complexes exhibit the LF bands at somewhat higher energy than the corresponding Fe compounds.[17] Spectra for the Ru complexes consist of a single absorption peak or a shoulder on the low-energy side of an intense absorption feature. The low-energy feature is assigned to the $a^1E_1 \leftarrow {}^1A_1$ transition in all cases.[16,17] Further analysis of the spin-allowed LF spectra of these complexes cannot be made because no other singlet–singlet LF absorption bands are observed. As in the Fe case, the Ru complexes with high solubility ($[(\eta^5\text{-}C_5H_5)Ru(\eta^6\text{-HMB})]PF_6$ and $[(\eta^5\text{-}C_5H_5)Ru(\eta^6\text{-}1,3,5\text{-}(t\text{-}Bu)_3C_6H_3)]PF_6$) exhibit weak absorption shoulders ($\lambda_{max} = 370$ nm ($\epsilon_{max} = 9$ M^{-1} cm^{-1}, CH_3CN) and $\lambda_{max} = 380$ nm ($\epsilon_{max} = 8$ M^{-1} cm^{-1}, CH_2Cl_2), respectively), which we assign to the $a^3E_1 \leftarrow {}^1A_1$ LF transition.

Long-Wavelength Irradiation and Sensitization of the Complexes. Irradiation of $[(\eta^5\text{-}C_5H_5)Fe(\eta^6\text{-}p\text{-xyl})]^+$ with 578- or 690-nm radiation (the region of singlet–triplet absorption ($\lambda_{max} = 650$ nm, $\epsilon_{max} = 1.5$ M^{-1} cm^{-1})) in CH_2Cl_2 solution containing 1,10-phenanthroline results in the release of *p*-xylene and the formation of $Fe(phen)_3^{2+}$. Due to the problems associated with actinometric measurements and the low extinction coefficients of the complex at these wavelengths, quantum yields were not determined.

Sensitization of the arene release reaction of $[(\eta^5\text{-}C_5H_5)Fe(\eta^6\text{-}p\text{-xyl})]^+$ occurs when triplet sensitizers present (benzil ($E_T = 532$ nm) and anthracene ($E_T = 680$ nm)[13]) are irradiated at 366 nm. Details of these experiments are given in the Experimental Section.

Irradiation of the Ru complex $[(\eta^5\text{-}C_5H_5)Ru(\eta^6\text{-}C_6H_6)]^+$ in acetonitrile solution at 406 nm (a region of singlet–triplet absorption) results in the formation of $[(\eta^5\text{-}C_5H_5)Ru(CH_3CN)_3]^+$. As in the case of the Fe complex, the low extinction coefficient of the complex precludes the accurate measurement of the quantum yield at this photolysis wavelength. Sensitization experiments were not conducted in the case of the Ru complexes.

(13) Morrison, W. H.; Ho, E. Y.; Hendrickson, D. N. *Inorg. Chem.* **1975**, *14*, 500.

(14) Here we adopt the nomenclature for identifying the electronic transitions from ref 15.

(15) (a) Scott, D. R.; Matsen, F. A. *J. Phys. Chem.* **1968**, *72*, 16. (b) Warren, K. D. *Inorg. Chem.* **1974**, *13*, 1243. (c) Clack, D. W.; Warren, K. D. *Struct. Bonding (Berlin)* **1980**, *39*, 1.

(16) The position and intensity of this transition are consistent with an analogous transition identified in ruthenocene.[17]

(17) Sohn, Y. S.; Hendrickson, D. N.; Gray, H. B. *J. Am. Chem. Soc.* **1971**, *93*, 3603.

Table V. Deuteration Effects on the Quantum Yield of Arene Release from $[(\eta^5\text{-}C_5H_5)M(\eta^6\text{-arene})]PF_6$

M	arene	ϕ^a	M	arene	ϕ^a
Fe[b]	toluene	0.39 (1)	Ru[c]	benzene	0.34 (1)
Fe[b]	toluene-d_8	0.35 (1)	Ru[c]	benzene-d_6	0.32 (1)

[a] Numbers in parentheses are the estimated standard deviations in the last significant digits. [b] Measured for CH_2Cl_2 solutions. [c] Measured for CH_3CN solutions.

Table VI. Temperature Dependence of Arene Release Quantum Yields

		CH_2Cl_2		CH_3CN	
M	arene	T, K	ϕ^a	T, K	ϕ^a
Fe[b]	*p*-xylene	293	0.58 (3)	293	0.71 (4)
		273	0.48 (2)	273	0.68 (5)
		253	0.37 (2)	253	0.62 (2)
		233	0.22 (3)	233	0.56 (4)
Fe[b]	hexamethylbenzene	293	0.054 (5)	303	0.43 (2)
		273	0.044 (3)	293	0.41 (2)
		253	0.030 (2)	273	0.38 (3)
		238	0.021 (2)	253	0.31 (2)
		233	0.017 (5)		
Ru[c]	benzene			313	0.37 (1)
				294	0.34 (1)
				273	0.30 (1)
				253	0.25 (1)

[a] Numbers in parentheses are the estimated standard deviations in the last significant digits. [b] BF_4^- salt. [c] PF_6^- salt.

Quantum Yields of Substituted Complexes. Irradiation of $[(\eta^5\text{-}C_5H_5)Fe(\eta^6\text{-arene})]^+$ at 436 nm in dichloromethane or acetonitrile solution leads to release of the arene and the production of $Fe(phen)_3^{2+}$. In contrast, 313-nm irradiation of $[(\eta^5\text{-}C_5H_5)Ru(\eta^6\text{-arene})]^+$ in dichloromethane solution gives no detectable reaction; however, acetonitrile solutions of the Ru complexes are photosensitive, yielding $[(\eta^5\text{-}C_5H_5)Ru(CH_3CN)_3]^+$ as the only Ru-containing product. The quantum yields under the conditions studied for the substituted complexes are given in Table IV. The magnitude of the quantum yield decreases with increasing alkyl substitution of the arene and decreases with an increase in the size of the alkyl substituent. Chloro substituents on the arene ring increase the quantum yield for arene release. The quantum yield determined for acetonitrile solutions of a given arene complex are always larger for the Fe complex than the corresponding Ru complex. In general, quantum yields are larger for a given Fe complex in acetonitrile than dichloromethane.

Quantum Yield Dependence on Arene Ring Deuteration. The quantum yields for arene release were investigated for $[(\eta^5\text{-}C_5H_5)Fe(\eta^6\text{-tol-}d_8)]PF_6$, $[(\eta^5\text{-}C_5H_5)Ru(\eta^6\text{-}C_6D_6)]PF_6$, and the protio analogues (see Table V). Deuteration of the arene decreases the quantum yield slightly for both metals from 0.39 (1) to 0.35 (1) for the Fe system and from 0.34 (1) to 0.32 (1) for the Ru system.

Quantum Yield Dependence on Temperature. The arene release quantum yields for $[(\eta^5\text{-}C_5H_5)Fe(\eta^6\text{-}p\text{-xyl})]BF_4$ and $[(\eta^5\text{-}C_5H_5)Fe(\eta^6\text{-HMB})]BF_4$ have been measured as a function of temperature in dichloromethane and acetonitrile solutions (Table VI). Data for $[(\eta^5\text{-}C_5H_5)Ru(\eta^6\text{-}C_6H_6)]PF_6$ were similarly obtained for acetonitrile solutions. Plots (vide infra) of $\log(\phi/(1-\phi))$ vs. $1/T$ for these data give straight lines from which $E_{a,p} - E_{a,nr}$ (slope) and $\log(A_p/A_{nr})$ (intercept) were extracted. These data are given in Table VII.

Medium Dependence of Arene Release from $[(\eta^5\text{-}C_5H_5)Fe(\eta^6\text{-HMB})]BF_4$ and $[(\eta^5\text{-}C_5H_5)Fe(\eta^6\text{-HEB})]^+$. The quantum yields (Table IX) for the release of the arene from $[(\eta^5\text{-}C_5H_5)Fe(\eta^6\text{-HEB})]^+$ in dichloromethane and acetonitrile solutions were measured in the presence of different counterions (BF_4^-, BPh_4^-, PF_6^-, AsF_6^-, SbF_6^-). The quantum yield for the hexaethylbenzene complex is always smaller than that found for the hexamethylbenzene complex under identical conditions. The quantum yield of the hexaethylbenzene complex in CH_2Cl_2 solutions varies with counterion in a manner similar to that found previously for the *p*-xylene complex. For the conditions studied, a limiting value of $\phi = 0.0007$ occurs for the hexaethylbenzene complex in CH_2Cl_2–0.1 M (TBA)AsF.

Table VII. Activation Parameters for Photochemical Arene Release from $[(\eta^5\text{-}C_5H_5)M(\eta^6\text{-arene})]^+$ [a]

M	arene	solvent	$\log(A_p/A_{nr})$	$E_{a,p} - E_{a,nr}$, kcal/mol
Fe[b]	*p*-xylene	CH_2Cl_2	2.8 (0.4)	3.6 (0.6)
Fe[b]	*p*-xylene	CH_3CN	1.5 (0.5)	1.5 (0.7)
Fe[b]	hexamethylbenzene	CH_2Cl_2	0.79 (0.2)	2.7 (0.3)
Fe[b]	hexamethylbenzene	CH_3CN	0.64 (0.3)	1.0 (0.5)
Ru[c]	benzene	CH_3CN	0.80 (0.4)	1.5 (0.5)

[a] Activation parameters are derived from plots of $\log(\phi/(1-\phi))$ vs. $1/T$. (see Appendix and the text for details). Fe compounds are BF_4^- salts; the Ru compound is a PF_6^- salt. Numbers in parentheses are estimated standard deviations. [b] −40 to +20 °C temperature range. [c] −20 to +40 °C temperature range.

Table VIII. Derived Values[a] of ρ and $\log(\phi_0/(1-\phi_0))$ for Cl- and CH_3-Substituted[b] $[(\eta^5\text{-}C_5H_5)M(\eta^6\text{-arene})]^+$ Complexes

M	solvent	ρ	$\log(\phi_0/(1-\phi_0))$	correln coeff
Fe[c]	CH_2Cl_2	+1.03	+0.48	+0.975
Fe[c]	CH_3CN	+0.53	+0.63	+0.982
Ru	CH_3CN	+1.38	−0.38	+0.996

[a] Values are derived from the slope (ρ) and the intercept ($\log(\phi_0/(1-\phi_0))$) of the plots of $\log(\phi/(1-\phi))$ vs. the Hammett σ_p parameter shown in Figures 1 and 2. [b] σ_p for Cl, +0.227; σ_p for CH_3, −0.17. [c] Data point for arene = hexamethylbenzene was not included in the least-squares analysis.

Table IX. Solvent and Counterion Effects on the Quantum Yield of Photochemical Arene Release from $[(\eta^5\text{-}C_5H_5)Fe(\eta^6\text{-HMB})]^+$ and $[(\eta^5\text{-}C_5H_5)Fe(\eta^6\text{-HEB})]^+$ [b]

anion	arene	conditions	ϕ^a
BF_4^-	HMB	CH_3CN	0.41 (1)
BF_4^-	HEB	CH_3CN	0.30 (1)
BF_4^-	HMB	CH_2Cl_2	0.035 (2)
BF_4^-	HEB	CH_2Cl_2	0.0044 (2)
BF_4^-	HEB	CH_2Cl_2/0.1 M (TBA)BF_4	0.0046 (1)
AsF_6^-	HEB	CH_2Cl_2	0.00088 (4)
AsF_6^-	HEB	CH_2Cl_2/0.1 M (TBA)AsF_6	0.00071 (1)
BPh_4^-	HEB	CH_2Cl_2	0.00080 (6)
SbF_6^-	HEB	CH_2Cl_2	0.00098 (1)
PF_6^-	HEB	CH_2Cl_2	0.00099 (1)

[a] Numbers in parentheses are the estimated standard deviations in the last significant digits. [b] Abbreviations: HMB = hexamethylbenzene, HEB = hexaethylbenzene.

Discussion

Identification and Nature of the Photoactive State. Photolysis of the Fe and Ru compounds in the region of the $a^3E_1 \leftarrow {}^1A_1$ spin-forbidden LF absorption band[14,15] results in the arene release reaction. Additionally for $[(\eta^5\text{-}C_5H_5)Fe(\eta^6\text{-}p\text{-xyl})]^+$, triplet sensitizers[11,12] (benzil, E_T = 18 800 cm^{-1}; anthracene, E_T = 14 700 cm^{-1}) with E_T near λ_{max} for the complex (λ_{max} = 650 nm; E = 15 400 cm^{-1}) efficiently sensitize the arene release reaction. These experimental data are all consistent with the lowest LF triplet excited state (a^3E_1) as the photoactive excited state in complexes of both metals. This a^3E_1 excited state (1e excitation $d_{z^2} \rightarrow (d_{xz}, d_{yz})$) is expected on theoretical grounds to have a weaker M–arene bond relative to that for the $^1A_1$ ground state,[18] where the M–arene bond

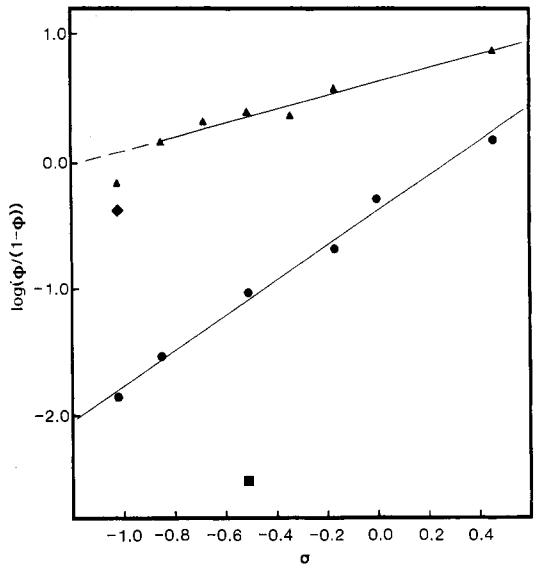

Figure 1. Plots of log $(\phi/(1-\phi))$ vs. σ_p (CH_3CN solution data) for chloro- and methyl-substituted $[(\eta^5\text{-}C_5H_5)Fe(\eta^6\text{-arene})]BF_4$ (▲) and $[(\eta^5\text{-}C_5H_5)Ru(\eta^6\text{-arene})]PF_6$ (●) complexes. The values of log $(\phi/(1-\phi))$ are derived from the quantum yield data in Table IV. The straight lines displayed are the least-squares lines with the appropriate slope and intercept values from Table VIII for complexes with less than six substituents. The points labeled ♦ and ■ are data points for $[(\eta^5\text{-}C_5H_5)Fe(\eta^6\text{-HEB})]BF_4$ and $[(\eta^5\text{-}C_5H_5)Ru(\eta^6\text{-}1,3,5\text{-}(t\text{-}Bu)_3C_6H_3)]PF_6$, respectively; these points were not included in the least-squares analyses.

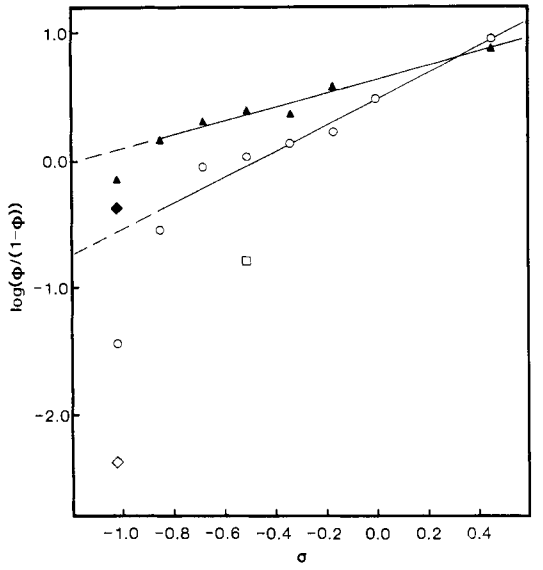

Figure 2. Plots of log $(\phi/(1-\phi))$ vs. σ_p for chloro- and methyl-substituted $[(\eta^5\text{-}C_5H_5)Fe(\eta^6\text{-arene})]BF_4$ in CH_3CN solution (▲) and in CH_2Cl_2 solution (○). The values of log $(\phi/(1-\phi))$ are derived from the quantum yield data in Table IV. The straight lines displayed are the least-squares lines with the appropriate slope and intercept values from Table VIII for complexes with less than six substituents. The points labeled ◇, ♦, and □ are data points for $[(\eta^5\text{-}C_5H_5)Fe(\eta^6\text{-HEB})]BF_4$ in CH_2Cl_2 and CH_3CN solution and $[(\eta^5\text{-}C_5H_5)Fe(\eta^6\text{-}1,3,5\text{-}(t\text{-}Bu)_3C_6H_3)]BF_4$ in CH_2Cl_2 solution, respectively; these points were not included in the least-squares analyses.

energies are estimated to be greater than 22 kcal/mol.[19,20]

Quenching[21] and low-temperature luminescence studies[21a,22] of ferrocene and ruthenocene (molecules with electronic structures closely analogous to the $[(\eta^5\text{-}C_5H_5)M(\eta^6\text{-arene})]^+$ compounds studied here) indicate that, in these complexes, the lowest metal-centered a^3E_1 excited state is highly distorted. For example, in ruthenocene, the distortion corresponds to a lengthening in the M–ring symmetric breathing mode[21a,22] and is quite large (10000 cm^{-1}). By analogy, the a^3E_1 excited state in the $[(\eta^5\text{-}C_5H_5)M(\eta^6\text{-arene})]^+$ complexes should be similarly distorted, weakening the M–arene bond and exposing the metal to nucleophilic attack. Spectroscopic experiments are currently in progress to investigate further the nature of the photoactive excited state.

Substituent Effects. As developed in the Appendix, the Hammett relationship[23] may be utilized to analyze the electronic and steric effects caused by arene ring substitutents. Implicit to the discussion[24] that follows is the hypothesis that variations of log $(\phi/(1-\phi))$ (a measure of k_p/k_{nr}, see Appendix) are due primarily to variations in k_p, the rate constant of arene release from the excited a^3E_1 state. The less likely possibility that decreases in the quantum yield with increased methyl substitution for a given metal might be photophysical in origin was considered (i.e., variations in k_{nr}, the rate constant for nonradiative decay of a^3E_1 back to $^1A_1$). By comparison of the quantum yields for arene release of otherwise analogous protio and deuterio complexes, some measure of the arene substituent effect on k_{nr} could be realized. The results of these studies are given in Table V. A slight decrease in ϕ occurs for complexes of both metals upon deuteration of the arene ring. k_{nr} for $a^3E_1 \rightsquigarrow {}^1A_1$ apparently changes little on substitution of D for H even though C–H (or C–D) bond stretching modes are commonly found to be efficient contributors to the magnitude of k_{nr}.[25] These results, along with the previously discussed large excited-state distortion predicted for these complexes in the M–arene bond coordinate, indicate that changes in the magnitude of k_{nr}[26] are more likely a function of the M–arene stretching mode frequency. Arene substitution is predicted to have only a minimal effect on this parameter.

(18) (a) Vanquickenborne, L. G.; Ceulemans, A. *J. Am. Chem. Soc.* **1977**, *99*, 2208. (b) Wrighton, M.; Gray, H. B.; Hammond, G. S. *Mol. Photochem.* **1973**, *5*, 165. (c) Zink, J. I. *J. Am. Chem. Soc.* **1974**, *96*, 4464.

(19) Our estimate of 22 kcal/mol for E_a of *p*-xylene release from $[(\eta^5\text{-}C_5H_5)Fe(\eta^6\text{-}p\text{-xyl})]BF_4$ is a lower limit of the Fe(II)–arene bond strength. Studies summarized in ref 20 indicate this bond strength may be as high as 50 kcal/mol.

(20) Connor, J. A. *Top. Curr. Chem.* **1977**, *71*, 71.

(21) (a) Wrighton, M. S.; Pdungsap, L.; Morse, D. L. *J. Phys. Chem.* **1975**, *79*, 66. (b) Fry, A. J.; Liu, R. S. H.; Hammond, G. S. *J. Am. Chem. Soc.* **1966**, *88*, 4781. (c) Farmilo, A.; Wilkinson, F. *Chem. Phys. Lett.* **1975**, *34*, 575. (d) Balzani, V.; Moggi, L.; Manfrin, M. F.; Bolletta, F.; Laurence, G. S. *Coord. Chem. Rev.* **1975**, *15*, 321. (e) Chapple, A. P.; Vikesland, J. P.; Wilkinson, F. *Chem. Phys. Lett.* **1977**, *50*, 81.

(22) Crosby, G. A.; Hager, G. D.; Hipps, K. W.; Stone, M. L. *Chem. Phys. Lett.* **1974**, *28*, 497.

(23) (a) McDaniel, D. H.; Brown, H. C. *J. Org. Chem.* **1958**, *23*, 420. (b) Ritchie, C. D.; Sager, W. F. *Prog. Phys. Org. Chem.* **1964**, *2*, 323. (c) Shorter, J. *Chem. Br.* **1969**, *5*, 269. (d) Hammett, L. P. "Physical Organic Chemistry", 2nd ed.; McGraw-Hill: New York, 1970.

(24) These arguments are based on an underlying view that the arene release reactions occur via attack of the medium on the a^3E_1 excited state. This formalism allows for *no deactivational steps after nucleophilic attack has occurred.* A *mathematically* equivalent formalism would allow *excited-state* deactivation and the additional deactivation step after nucleophilic attack. The experimental data in hand do not allow us to determine which of these formalisms are in fact correct descriptions of the system. With these ambiguities in mind, we have chosen the former (one deactivational step) case for constructing our discussion of the reaction mechanism. The observation of emissive behavior from the reactive excited state in this system would be extremely useful for resolving these ambiguities.

(25) An excellent discussion of hydrogen isotope effects in the photophysics of transition-metal systems has recently been published. See: Graff, J. L.; Wrighton, M. S. *J. Am. Chem. Soc.* **1981**, *103*, 2225 and references therein.

(26) Clearly, k_{nr} should increase substantially for the Ru analogues (k_{nr}(Ru) > k_{nr}(Fe)) because of the larger spin–orbit coupling constant exhibited by Ru. This prediction is supported by the smaller values of log $(\phi/(1-\phi))$ measured for the Ru analogues in each case.

In Figure 1, plots of log $(\phi/(1-\phi))$ vs. σ_p for arene release are shown for a series of substituted-arene Fe and Ru complexes in CH_3CN solution. Least-squares analyses for data obtained on methyl- and chloro-substituted complexes (up to and including five subsituents for Fe; up to and including six substituents for Ru) indicate there is a good, linear correlation between log $(\phi/(1-\phi))$ and σ_p for both metals. Derived values for ρ, the reaction constant, are given in Table VIII. The straight-line behavior exhibited by these plots indicate that inductive electronic effects determine the variation of the quantum yield with substituent for the chloro- and methyl-substituted compounds in CH_3CN solution. The relatively low, positive values obtained for ρ in both metal systems ($\rho = +0.53$ for Fe and $\rho = +1.38$ for Ru) are consistent with the development of a small amount of negative charge at the arene in the transition state. These small changes in charge separation are consistent with the metal-localized nature of the a^3E_1 LF excited state from which the arene release reaction occurs. The larger ρ value found for the Ru system coincides with the expected increase in the covalency of the Ru–arene bond in comparison to that of the Fe–arene bond.

Data obtained for the compounds in CH_2Cl_2 solution show more interesting and diverse behavior (Figure 2). None of the Ru complexes show any indication of arene release in CH_2Cl_2 solution, confirming previous observations: the role of the solvent (nucleophilicity) is even more crucial for the arene release reactions in the Ru systems than in the previously studied $[(\eta^5\text{-}C_5H_5)Fe(\eta^6\text{-}p\text{-xyl})]^+$ complex. In contrast to the Ru results, photochemical arene release in CH_2Cl_2 *does* occur for all the Fe compounds studied, enabling the correlation of log $(\phi/(1-\phi))$ with σ_p to be investigated as a function of solvent. Figure 2 shows plots for log $(\phi/(1-\phi))$ vs. σ_p for CH_3CN and CH_2Cl_2 solutions of the Fe complexes.

The CH_2Cl_2 solution data (up to and including five substituents) give a linear correlation as in the acetonitrile case. The ρ value of +1.03 indicates slightly more negative charge buildup at the arene in the transition state than in the acetonitrile case, perhaps as a consequence of the lower dielectric constant of CH_2Cl_2. For six substituents, the linear correlation begins to break down, with the sixth methyl group causing a much larger decrease in log $(\phi/(1-\phi))$ than would be predicted from the linear $n = 0$–5 data. This behavior suggests that, in CH_2Cl_2, steric effects become the important factors in determining the rate of arene release.

To investigate these steric effects further, complexes containing larger alkyl substituents (ethyl, *tert*-butyl) with σ_p values similar to that of methyl were investigated. Arenes studied included tri-*tert*-butylbenzene and the extremely bulky hexaethylbenzene. The spectroscopic properties of complexes containing these arenes are in all cases similar to those found for the methyl-substituted derivatives. The bulky substituents in these complexes do not significantly decrease the ground- or excited-state stability of the M–arene bond but quite dramatically influence the stability of the transition state for arene release. Data for the most hindered Fe complexes (BF_4^- salts) are given in Table IX. In CH_3CN solutions, a small decrease of ϕ from 0.41 (arene = hexamethylbenzene) to 0.30 (arene = hexaethylbenzene) occurs. The analogous quantum yields determined for CH_2Cl_2 solutions show a larger effect, with quantum yields of 0.035 and 0.0044, respectively. A similar trend occurs for the mesitylene and 1,3,5-tri-*tert*-butylbenzene Fe complexes in CH_2Cl_2 solution ($\phi = 0.52$ and 0.14, respectively). These results are consistent with our previous investigation[2] of media effects in arene release from $[(\eta^5\text{-}C_5H_5)Fe(\eta^6\text{-}p\text{-xyl})]^+$. Bulky alkyl substituents are effective in blocking the weak nucleophile BF_4^- from participating in the transition state but are much less effective at blocking the good nucleophile CH_3CN. In the analogous Ru complexes, a larger decrease is exhibited for CH_3CN solution quantum yield data between the mesitylene and 1,3,5-tri-*tert*-butylbenzene complexes ($\phi = 0.085$ and 0.0031, respectively). The nucleophilicity of the medium makes a more important contribution to the transition state of the arene release reaction for Ru–arene complexes.

Table X. Conductivity Measurements for $[(\eta^5\text{-}C_5H_5)Fe(\eta^6\text{-HEB})]^+$ Salts in Dichloromethane Solution at 25 °C

anion	concn, M	Λ, Ω^{-1} cm^{-1} mol^{-1} [a]	anion	concn, M	Λ, Ω^{-1} cm^{-1} mol^{-1} [a]
BF_4^-	0.02	22	AsF_6^-	0.002	38
BPh_4^-	0.02	26	AsF_6^-	0.0002	67
AsF_6^-	0.02	25			

[a] Estimated standard deviations are 5%.

Temperature Effects. To gain a better understanding of the relative importance of the enthalpy and entropy contributions required to assemble the transition state for the photochemical arene release from a^3E_1, the temperature dependence of the kinetic parameter k_p/k_{nr} was investigated. The results of these studies are given in Table VI.

The Appendix outlines the method we have chosen for data analysis. Essentially, this analysis predicts that a plot of log $(\phi/(1-\phi))$ vs. $1/T$ should yield a straight line with a slope of $E_{a,p} - E_{a,nr}$ and an intercept of log (A_p/A_{nr}). This behavior is found for each set of experimental data obtained over a 60 deg temperature range. As can be seen from the derived data in Table VII, $E_{a,p} - E_{a,nr}$ is small (1.0–3.6 kcal/mol) for all the systems studied. If $E_{a,nr}$ is considered to be at most several kilocalories per mole, $E_{a,p}$ values, the apparent activation energies for arene release from a^3E_1, are on the order of 2–7 kcal/mol. Relatively small enthalpies of activation are necessary to take the a^3E_1 excited-state geometry to the activated complex for arene release. The ground-state M–arene bond energies of >22 kcal/mol are substantially reduced in the a^3E_1 excited state. Differences between $E_{a,p} - E_{a,nr}$ for $[(\eta^5\text{-}C_5H_5)Fe(\eta^6\text{-}p\text{-xyl})]^+$ and $[(\eta^5\text{-}C_5H_5)Fe(\eta^6\text{-HMB})]^+$ complexes show an interesting trend. In both solvents studied $E_{a,p} - E_{a,nr}$ is larger for the *p*-xylene complex than for the hexamethylbenzene complex. This is the opposite order predicted from trends in Fe–arene bond strengths. A similar pattern has been observed for E_a in the thermal arene release reactions of $(arene)Cr(CO)_3$ and has been briefly discussed.[27]

For both Fe complexes studied, $E_{a,p} - E_{a,nr}$ and log (A_p/A_{nr}) are larger for CH_2Cl_2 solution data than CH_3CN data. The enthalpic portion of the interaction between the a^3E_1 excited state and its environment is more favorable in CH_3CN, but the entropic part of the interaction is more favorable in CH_2Cl_2. Further molecular interpretations of these data are unwarranted until independent measurements of the temperature dependence of either k_p or k_{nr} can be made.

Medium Effects on ϕ for $[(\eta^5\text{-}C_5H_5)Fe(\eta^6\text{-HEB})]^+$. Because our original hypotheses in the area of M–arene photochemistry included the possibility of observing a purely dissociative arene release from a metal–arene complex, we have investigated the effect of the medium on the quantum yield for arene release from the sterically hindered Fe compounds. If *all* media-assisted pathways of excited-state arene release are stopped, then any remaining photochemical arene release observed would result *only* from a purely dissociative step. The data in Table IX indicate an apparently limiting value of $\phi = 0.0007$ is reached for the release of arene from $[(\eta^5\text{-}C_5H_5)Fe(\eta^6\text{-HEB})]^+$ in CH_2Cl_2 solutions containing the weak nu-

(27) (a) Muetterties, E. L.; Bleeke, J. R.; Wucherer, E. J.; Albright, T. A. *Chem. Rev.* **1982**, *82*, 499.

cleophile AsF_6^-. This low value is not due to a decrease in the ion-pairing constants for $[(\eta^5\text{-}C_5H_5)Fe(\eta^6\text{-HEB})]^+X^-$ relative to those found for $[(\eta^5\text{-}C_5H_5)Fe(\eta^6\text{-}p\text{-xyl})]^+X^-$ (conductivity data, Table X) but may signify that the medium-assisted pathways have indeed been stopped. A definitive statement that 0.0007 for ϕ is a limiting value for dissociative arene release cannot be made because this value may still contain a nucleophilic component due to attack by the solvent CH_2Cl_2.

Conclusions

The photochemical removal of arenes from several Fe(II) and Ru(II) complexes of the general form $[(\eta^5\text{-}C_5H_5)M(\eta^6\text{-arene})]^+$ has been studied as a function of arene and temperature. The photoactive state in these systems is the distorted a^3E_1 LF excited state. For chloro- and methyl-substituted arenes a linear correlation exists between log $(\phi/(1-\phi))$ and σ_p. The small, positive ρ values found for the correlations reveal a small amount of negative charge builds up at the arene in the transition state. Sterically hindered arenes give log $(\phi/(1-\phi))$ values that are smaller than those predicted from the linear methyl- and chloro-substituted complex data. The sterically hindered arenes hexamethylbenzene, hexaethylbenzene, and 1,3,5-tri-*tert*-butylbenzene diminish solvent cage participation in the transition state for arene release.

Plots of log $(\phi/(1-\phi))$ vs. $1/T$ give linear plots that yield the difference in apparent activation energies $(E_{a,p} - E_{a,nr})$ between the arene release step and nonradiative decay of the a^3E_1 excited state. The small values of this parameter (1–4 kcal/mol) compared with the ground-state M–arene bond energies of >25 kcal/mol are consistent with nearly complete M–arene bond cleavage in the a^3E_1 excited state.

A limiting value of $\phi = 0.0007$ is reached for arene release from $[(\eta^5\text{-}C_5H_5)Fe(\eta^6\text{-HEB})]^+$ in dichloromethane solutions containing the weak nucleophile AsF_6^-. This value is an upper limit for dissociative arene release in the Fe system.

During the past several years, we have concentrated our efforts to obtain an understanding of photochemical arene release in simple systems, which contain only polydentate ligands. Experiments are now in progress to extend these studies to other M–arene systems (e.g., those that contain monodentate ligands), to determine the generality of this class of photochemical reactions, and to explore the potential of the photogenerated reactive intermediates as photoassistance agents.

Acknowledgment. We wish to thank Professor H. B. Gray for several helpful discussions, Dr. M. C. Palazzotto for assistance in carrying out the conductivity measurements, and W. Hollenberg for making several preliminary quantum yield measurements. This research was supported in part by a grant from the Department of Energy. The Cary Model 17-D spectrometer was made available by funding received in part from the National Science Foundation (Grant CHE 78-23857).

Appendix

The interpretation of the quantum yield data developed in the text is based on a general model developed previously for the photoreactions of low-spin d^6 complexes[27] ($[Co(NH_3)_6]^{3+}$, $[Rh(NH_3)_6]^{3+}$, and $[Rh(NH_3)_5Cl]^{2+}$).

The overall quantum yield ϕ_p for product formation is given by eq 3, where ϕ_{p,T_1} = the quantum yield of product from the

$$\phi_p = \phi_{p,T_1}\phi_{isc} \tag{3}$$

reactive excited state and ϕ_{isc} = the quantum yield for intersystem crossing from the lowest lying singlet excited state to the reactive excited state. By definition

$$\phi_p = k_p/(k_p + k_{nr,T_1} + k_{r,T_1}) \tag{4}$$

$$\phi_{isc} = k_{isc}/(k_{isc} + k_{nr,S_1} + k_{r,S_1}) \tag{5}$$

where k_p is the rate of product formation from the reactive excited state, k_{nr,T_1} and k_{nr,S_1} are the rate constants for *nonradiative* decay from T_1 and S_1, k_{r,T_1} and k_{r,S_1} are the rate constants for *radiative* decay from T_1 and S_1, and k_{isc} is the rate constant for intersystem crossing from S_1 to T_1.

In general, each rate constant may vary for each metal complex with metal, arene, counterion, solvent, etc.; however, due to the close similarities of the complexes studied, several reasonable assumptions can be made to allow further analysis of the quantum yield data: k_{r,T_1} and k_{r,S_1} can be neglected because no phosphorescence or fluorescence is observed for any of the complexes under the conditions of the photochemical measurements. Additional simplification results for ϕ_p if ϕ_{isc} is assumed to be approximately constant for all the complexes studied for a given metal. It is quite likely, on the basis of previous observations for d^6 metal complexes and the high values of ϕ measured here (see text), that $\phi_{isc} \approx 1$ for *all* the complexes.[28] The expression for ϕ_p simplifies to

$$\phi_p = \phi = \phi_{p,T_1} = k_p/(k_p + k_{nr,T_1}) \tag{6}$$

Rearrangement of eq 6 gives

$$k_p/k_{nr,T_1} = k_p/k_{nr} = \phi/(1-\phi) \tag{7}$$

Only the ratio of k_p to k_{nr} can be determined without an independent rate measurement of either k_p or k_{nr}; however, for the closely related series of complexes studied here, it is very likely that k_{nr} is nearly constant for *all the complexes of a given metal*. Some experimental justification for this assumption is available from the small effect observed on ϕ when the arene ring is deuterated (see Table V), because a prevalent nonradiative decay mode observed for metal complexes involves the high-energy C–H stretching modes. Finally, even if k_{nr} is not constant for all the complexes of a given metal, any variations are expected to be small and systematic for the arenes studied.

In summary, this theoretical treatment equates the experimentally derived expression $\phi/(1-\phi)$ with k_p/k_{nr} and subsequently allows the quantity $\phi/(1-\phi)$ to be treated as an empirical rate parameter which contains chemically significant information concerning the arene release reactions studied. Additionally, k_p may be a pseudo-first-order rate constant that imparts media dependence to $\phi/(1-\phi)$ without destroying the general result. We have used the ratio $\phi/(1-\phi)$ in two data treatments commonly employed with rate constant measurements: linear free energy correlations and temperature dependence.

Hammett Relationship

$$\log(\phi/(1-\phi)) = \log(k_p/k_{nr}) = \rho\sigma_p + \log(k_{o,p}/k_{o,nr}) \tag{8}$$

$$\sigma_p = \text{substituent constant} \tag{9}$$

$$\rho = \text{reaction constant} \tag{10}$$

$$k_{o,p}/k_{o,nr} = \phi/(1-\phi) \text{ for unsubstituted complex} \tag{11}$$

(28) (a) Adamson, A. W.; Fleischauer, P. D. "Concepts of Inorganic Photochemistry"; Wiley-Interscience: New York, 1975; pp 215–217. (b) Bergkamp, M. A.; Watts, R. J.; Ford, P. C. *J. Am. Chem. Soc.* **1980**, *102*, 2627.
(29) Demas, J. N.; Taylor, D. G. *Inorg. Chem.* **1979**, *18*, 3177.

Arrhenius Relationship

$$k_p = A_p \exp(-E_{a,p}/RT) \quad (12)$$

$$k_{nr} = A_{nr} \exp(-E_{a,nr}/RT) \quad (13)$$

$$\log (k_p/k_{nr}) = \log (A_p/A_{nr}) - ((E_{a,p} - E_{a,nr}/2.3RT) \quad (14)$$

$$\log (\phi/(1-\phi)) \text{ vs. } 1/T$$

$$\text{slope} = -(E_{a,p} - E_{a,nr})/2.3R \quad (15)$$

$$\text{intercept} = \log (A_p/A_{nr}) \quad (16)$$

Registry No. $[(\eta^5\text{-}C_5H_5)Fe(\eta^6\text{-}p\text{-}Cl_2C_6H_4)]^+$, 51150-13-1; $[(\eta^5\text{-}C_5H_5)Fe(B)]^+$ (B = η^6-chlorobenzene), 32965-46-1; $[(\eta^5\text{-}C_5H_5)Fe(\eta^6\text{-}C_6H_6)]^+$, 51364-24-0; $[(\eta^5\text{-}C_5H_5)Fe(\eta^6\text{-tol})]^+$, 32760-28-4; $[(\eta^5\text{-}C_5H_5)Fe(\eta^6\text{-}p\text{-xyl})]^+$, 32731-70-7; $[(\eta^5\text{-}C_5H_5)Fe(\eta^6\text{-mes})]^+$, 32757-50-9; $[(\eta^5\text{-}C_5H_5)Fe(B)]^+$ (B = η^6-durene), 62971-97-5; $[(\eta^5\text{-}C_5H_5)Fe(\eta^6\text{-PMB})]^+$, 62971-98-6; $[(\eta^5\text{-}C_5H_5)Fe(\eta^6\text{-HMB})]^+$, 54688-69-6; $[(\eta^5\text{-}C_5H_5)Fe(\eta^6\text{-}1,3,5\text{-}(t\text{-Bu})_3C_6H_3)]^+$, 90867-12-2; $[(\eta^5\text{-}C_5H_5)Fe(\eta^6\text{-HEB})]^+$, 71713-62-7; $[(\eta^5\text{-}C_5H_5)Fe(\eta^6\text{-}p\text{-xyl})]\text{-}CF_3SO_3$, 90867-13-3; $[(\eta^5\text{-}C_5H_5)Fe(\eta^6\text{-}p\text{-xyl})]PF_6$, 34978-37-5; $[(\eta^5\text{-}C_5H_5)Fe(\eta^6\text{-}p\text{-xyl})]AsF_6$, 90867-14-4; $[(\eta^5\text{-}C_5H_5)Fe(\eta^6\text{-}p\text{-xyl})]SbF_6$, 90867-15-5; $[(\eta^5\text{-}C_5H_5)Fe(\eta^6\text{-}p\text{-xyl})]BF_4$, 74176-24-2; $[(\eta^5\text{-}C_5H_5)Fe(\eta^6\text{-tol})]PF_6$, 33435-42-6; $[(\eta^5\text{-}C_5H_5)Fe(\eta^6\text{-tol-}d_8)]PF_6$, 90867-17-7; $[(\eta^5\text{-}C_5H_5)Fe(\eta^6\text{-HEB})]PF_6$, 71713-63-8; $[(\eta^5\text{-}C_5H_5)\text{-}Fe(\eta^6\text{-HEB})]AsF_6$, 90867-18-8; $[(\eta^5\text{-}C_5H_5)Fe(\eta^6\text{-HEB})]SbF_6$, 90867-19-9; $[(\eta^5\text{-}C_5H_5)Fe(\eta^6\text{-HEB})]BPh_4$, 90867-20-2; $[(\eta^5\text{-}C_5H_5)\text{-}Fe(\eta^6\text{-HEB})]BF_4$, 90867-21-3; $[(\eta^5\text{-}C_5H_5)Ru(\eta^6\text{-}p\text{-}Cl_2C_6H_4)]PF_6$, 80049-71-4; $[(\eta^5\text{-}C_5H_5)Ru(\eta^6\text{-}C_6H_6)]PF_6$, 72812-91-0; $[(\eta^5\text{-}C_5H_5)\text{-}Ru(\eta^6\text{-tol})]PF_6$, 78618-95-8; $[(\eta^5\text{-}C_5H_5)Ru(\eta^6\text{-mes})]PF_6$, 72804-52-5; $[(\eta^5\text{-}C_5H_5)Ru(\eta^6\text{-PMB})]PF_6$, 90867-23-5; $[(\eta^5\text{-}C_5H_5)Ru(\eta^6\text{-HMB})]PF_6$, 72804-78-5; $[(\eta^5\text{-}C_5H_5)Ru(\eta^6\text{-}1,3,5\text{-}(t\text{-Bu})_3C_6H_3)]PF_6$, 90867-25-7.

Contribution from the Research Institute for Materials, Faculty of Science, University of Nijmegen, Toernooiveld, 6525 ED Nijmegen, The Netherlands

Molecular Orbital Analysis of the Bonding in Gold Tertiary Phosphine Clusters and Their ^{197}Au Mössbauer Spectra

J. W. A. VAN DER VELDEN* and Z. M. STADNIK†

Received August 16, 1983

Extended Hückel molecular orbital calculations have been used in the analysis of the bonding in some mononuclear gold(I) compounds and in a series of gold clusters with monodentate tertiary phosphines. The nature of the metal–metal bond in gold clusters is discussed in terms of calculated overlap populations, which correlate well with crystallographically determined bond distances. Furthermore, an empirical correlation has been established between the Au(6p) electron population and the ^{197}Au Mössbauer quadrupole splitting, providing a better understanding of the ^{197}Au Mössbauer spectra of gold clusters. An explanation is provided for the absence of a separate signal for the central Au atom in the $[Au_9(PPh_3)_8]^{3+}$ and $[Au_8(PPh_3)_7]^{2+}$ clusters.

Introduction

Extended Hückel molecular orbital (EHMO) calculations on the bare skeletons of the $[Au_6]^{2+}$ and the $[Au_9]^{3+}$ clusters have shown that the Au(6s) orbitals dominate the bonding.[1] The dominant role of the Au(6s) orbitals in the bare gold clusters is caused by (i) the large 6s–6p energy separation, which makes hybridization for gold less attractive as compared with that for Cu, Ag, and other transition metals, and (ii) the strong contraction of the Au(5d) orbitals. These observations induced Mingos[1] and Vollenbroek et al.[2] to carry out Hückel calculations in which only 6s–6s overlaps between adjacent gold atoms were considered. This resulted in a similar energy level ordering as in the EHMO calculation and in a successful prediction of the ionic charge on the bare gold skeletons.[1,2] To study the effect of the coordination of ligands to a bare metal skeleton, also an EHMO calculation was performed on $[Au_6L_6]^{2+}$ (L = tertiary phosphine).[1] One filled atomic orbital (AO) was used per ligand, in correspondence with the lone pair donated by the tertiary phosphine upon coordination. From this calculation it was concluded that coordination of ligands to the bare metal skeleton of the $[Au_6]^{2+}$ cluster favors in-pointing hybridization of the metal orbitals. This result was, however, generalized for the larger centered gold clusters, resulting in strong radial and weak peripheral interactions.

In this report we describe the results of EHMO calculations on some mononuclear Au(I) compounds and a series of gold cluster compounds taking into account for the gold atoms the Au(5d), -(6s), and -(6p) AO's. The phosphine ligands were substituted by PH_3 units, taking into account the P(3s), -(3p) and H(1s) AO's (Table I). These calculations give an insight into the metal skeleton bonding. They show the importance of the peripheral interactions vs. the radial interactions in centered gold clusters, which has been a point of discussion.[3] Also the absence of a separate signal for the central gold atom in $[Au_9(PPh_3)_8]^{3+}$ and $[Au_8(PPh_3)_7]^{2+}$ in the ^{197}Au Mössbauer spectra has been subject to discussion. It has been postulated that for some reason its intensity might be too low to be

Table I. Parameters Used in the Extended Hückel Molecular Orbital Calculations

atom	orbital	Slater exponent (ζ)	H_{ii}, eV
H	1s	1.00	−13.60
P	3s	1.89	−18.77
	3p	1.63	−10.12
Cl	3s	2.36	−25.27
	3p	2.04	−13.69
Br	4s	2.64	−24.03
	4p	2.26	−12.35
I	5s	2.68	−20.62
	5p	2.32	−10.45
Au	6s	2.60	−9.22
	6p	2.58	−4.28
	5d	6.16 (ζ_1), 0.685 (c_1) 2.79 (ζ_2), 0.570 (c_2)	−10.97

† On leave from the Institute of Physics, Jagiellonian University, Cracow, Poland.

(1) D. M. P. Mingos, *J. Chem. Soc., Dalton Trans.*, 1163 (1976).
(2) F. A. Vollenbroek, J. J. Bour, and J. W. A. van der Velden, *Recl. Trav. Chim. Pays-Bas*, **99**, 137 (1980).
(3) J. J. Steggerda, J. J. Bour, and J. W. A. van der Velden, *Recl. Trav. Chim. Pays-Bas*, **101**, 164 (1982), and references therein.

0020-1669/84/1323-2640$01.50/0 © 1984 American Chemical Society